

# A Novel Tetrahedral Formally Zerovalent-Palladium Hydrido Complex Stabilized by Divalent Alkaline Earth Counterions

Malin Olofsson-Mårtensson, Mikael Kritikos, and Dag Noréus\*

Contribution from the Department of Structural Chemistry, Arrhenius Laboratory, Stockholm University, S-10691 Stockholm, Sweden

Received April 1, 1999

**Abstract:** To investigate how formally low-valent transition-metal hydrido complexes are stabilized without the conventional “back-donation mechanism” of electron density to ligand orbitals, a new tetrahedral formally zerovalent-palladium hydrido complex has been synthesized and structurally characterized in  $\text{Sr}_2\text{PdH}_4$  and  $\text{Ba}_2\text{PdH}_4$ . The two isomorphous hydrides were synthesized by hot sintering of the binary alkaline-earth hydride with palladium powder at temperatures close to 750 °C. The structures were determined to be of  $\beta\text{-K}_2\text{SO}_4$  type by means of X-ray single-crystal diffraction complemented by neutron powder diffraction from the corresponding deuteride. The structure can be described as consisting of tetrahedral palladium hydrido complexes and alkaline earth counterions. But the hydrides are also not far from being of an interstitial type, with hydrogen slightly off-center toward palladium from the octahedral interstices coordinating one palladium and five alkaline-earth atoms. This intermediate character is reflected in long Pd–H distances in the complex, averaging 1.80 Å in  $\text{Ba}_2\text{PdH}_4$  and 1.78 Å in  $\text{Sr}_2\text{PdH}_4$ . It also emphasizes the importance of the counterion contribution to the stabilization of these unusual, formally low oxidation states.

## Introduction

Metal hydrides containing transition metal (TM)–hydrogen complexes, with the transition metal in a formally low oxidation state, are of fundamental interest for clarifying how an electron-rich metal atom can be stabilized without access to the conventional mechanism for relieving the electron density by “back-donation” to suitable ligand orbitals. The detection and subsequent characterization of these systems is providing new insights into the metal–hydrogen bond mechanism in TM compounds, which might also make it possible to synthesize improved hydrogen storage systems for practical use.

Hydrogen binds to most metals, forming binary hydrides with hydrogen atoms in the tetrahedral and/or octahedral interstitial sites of an often more or less close-packed metal atom framework.<sup>1</sup> The physical properties vary greatly across the periodic table, mainly depending on the differences in electronegativity of the metal atoms from hydrogen. Connected with this is also the unique softness of hydrogen, as described for example by Pearson, which is expressed as a very low resistance to deformation of the electron density.<sup>2</sup> The relatively low electron affinity of hydrogen, as compared to, e.g., oxygen or the halogens, makes the electronic properties of the metal atoms more dominating in the bonding. One might say that the unique property of hydrogen, with its low electron affinity from filling the K shell, differentiates hydrides from other compounds where the energy gain from filling a conventional octet more strongly localizes the electrons.

By alloying, it has empirically been found that the metal–hydrogen bond strength can be so adjusted that hydrogen can be absorbed and released at temperatures close to ambient. This

has opened up the opportunity for the so-called hydrogen storage alloys presently being applied as electrode materials in rechargeable nickel–metal hydride batteries (NiMH).<sup>3</sup> Typical examples are systems such as  $\text{LaNi}_5$ ,  $\text{TiMn}_2$ , and  $\text{TiNi}$ , where a more electropositive metal, forming a stable binary hydride, is alloyed with a more electronegative transition metal to the right in the periodic table, which usually does not form a stable binary hydride. The resulting alloy hydrides are still of an interstitial type, with hydrogen in the tetrahedral and/or octahedral interstitial sites. Interactions with neighboring metal atoms determine the stability of the metal–hydrogen bond and thus the hydrogen adsorption/desorption pressure of the system. The fine-tuning of the hydrogen storage properties of commercial alloys typically involves a mixture of several metals.

The low metal–hydrogen bond strength, which also is a prerequisite for useful hydrogen storage systems, and short-range hydrogen–hydrogen repulsion effects exclude some of the interstitial sites from simultaneously being occupied, and the overall hydrogen storage capacity is usually below one hydrogen per metal atom (H/M) in commercial hydrides.

By reacting electropositive alkali or alkaline earth metals (s-elements) with group VII, VIII, IX, and X transition metals in the presence of hydrogen, a large number of interesting ternary and quaternary complex transition metal hydrides have been synthesized in the latest twenty years.<sup>4</sup> Although none of the transition metals forms stable binary hydrides, except for palladium, the hydrides based on the hydrogen-rich TM complexes have a considerably higher storage capacity than the now commercially available hydrogen storage alloys.

In the synthesis of these new hydrides, the electropositive s-elements are supplying their valence electrons to allow for

\* Address correspondence to this author.

(1) Mackay, K. M. *Hydrogen Compounds of the Metallic Elements*; Barnes and Nobles, Inc.: New York, 1966.

(2) Pearson, R. G. *Inorg. Chem.* **1988**, 27, 734–740.

(3) Sakai, T.; Matsuoka, M.; Iwakura, C. *Handbook on the Physics and Chemistry of Rare Earths*; Elsevier Science B.V.: Amsterdam, 1995; Vol. 21, p 133–178.

(4) Yvon, K. *Encyclopedia of Inorganic Chemistry*; King, B., Ed.; John Wiley & Sons Ltd: Chichester, England, 1994; Vol. 3.

the formation of usually 18-electron homoleptic TM–hydrogen complexes. TM–hydrogen complexes with 16, 14, and even 17 electrons have also been identified, leading to a puzzling variety of compositions, transition metal coordination numbers, and coordination geometries. Some are further complicated by having hydrogen bonded both in transition metal complexes and in interstitial sites coordinated by the s elements in structural building blocks similar to the binary s element hydrides. In a recent article in this journal, Firman and Landis have used their development of a local valence bond concept to rationalize the structure and coordination of most of these new hydrides.<sup>5</sup>

The TM–hydrogen bonds in complex transition metal hydrides are strong, thus making them unsuitable for hydrogen storage applications. A possible way of finding hydrides that are less stable with respect to the metal hydrogen bond would be to look for systems based on TM–hydrogen complexes with the lowest formal oxidation state on the transition metal. The stabilization of formally low oxidation states is usually connected with certain electron-accepting properties of the ligand, i.e., it should be a  $\pi$ -acid with unoccupied orbitals available. In the homoleptic TM–hydrogen complexes this stabilization cannot be realized. Some kind of stabilization mechanism is clearly operative, however, as a small number of electron-dense TM–H complexes have already been found, namely  $\text{Mg}_2\text{NiH}_4$ ,  $\text{Mg}_3\text{RuH}_3$ ,  $\text{Li}_2\text{PdH}_2$ , and  $\text{Na}_2\text{PdH}_2$ .<sup>6–9</sup> These systems are also interesting as such, since some of them exhibit unexpected metallic properties or intriguing lattice defects. The flexibility inherent in the polarizable TM–H bond and lattice-induced effect seems to offer enough relief of the high electron density in the  $d^{10}$  state of the central atom, helping to stabilize a formally oxidation state that is usually found only with good electron-accepting ligands. Again, palladium seems to even favor such a low oxidation state, as it has been found with a formal oxidation state of zero in two complexes: a linear  $\text{PdH}_2$  complex in  $\text{Li}_2\text{PdH}_2$  and  $\text{Na}_2\text{PdH}_2$  and a planar trigonal  $\text{PdH}_3$  complex in  $\text{NaBaPdH}_3$ .<sup>10</sup>

For comparison, an assumedly more conventional square-planar  $\text{Pd}^{\text{II}}\text{H}_4$  complex was only recently synthesized in  $\text{Na}_2\text{PdH}_4$ , but at an extreme 2000 bar  $\text{H}_2$  pressure.<sup>11</sup> Here we want to report another new  $\text{PdH}_4$  palladium hydrido complex with formally zerovalent palladium, found in  $\text{Ba}_2\text{PdH}_4$  and  $\text{Sr}_2\text{PdH}_4$ . Interestingly, it is among these formally low-valent systems that the prediction from the valence bond model encounters difficulties, and we want to argue that the understanding of the counterion contribution must be further developed for these systems. This also implies that by manipulating the counterion lattice, it should be possible to modify the TM–hydrogen bond strength, and as will be discussed below this might be used for creating practically useful hydrogen storage systems if the nickel analogues are synthesized.

## Experimental Section

**Syntheses.** To prevent samples and starting materials from undergoing oxidation they were stored and handled in an argon-filled glovebox.

(5) Firman, T. K.; Landis, C. L. *J. Am. Chem. Soc.* **1998**, *120*, 12650–12656.

(6) Zolliker, P.; Yvon, K.; Jørgensen, D.; Rotella, F. J. *Inorg. Chem.* **1986**, *25*, 3590–3593.

(7) Bonhomme, F.; Yvon, K.; Fischer, P. *J. Alloys. Comput.* **1992**, *186*, 309–314.

(8) Kadir, K.; Noréus, D. *Z. Phys. Chem. N.F.* **1989**, *163*, 231–232.

(9) Noréus, D.; Törnroos, K. W.; Börje, A.; Szabó, T.; Bronger, W.; Spittank, H.; Auffermann, G.; Müller, P. *J. Less Common Met.* **1988**, *139*, 233–239.

(10) Olofsson, M.; Kritikos, M.; Noréus, D. *Inorg. Chem.* **1998**, *37*, 2900–2902.

(11) Bronger, W.; Auffermann, G. *J. Alloys Compd.* **1995**, *228*, 119–121.

Cold-pressed powders of  $\text{BaH}_2$  or  $\text{SrH}_2$  and Pd in a 2:1 ratio were hot sintered in an  $\text{Al}_2\text{O}_3$  crucible under a hydrogen pressure of 40 bar during 2 days. In the temperature region between 710 and 730 °C, dark brown single  $\text{Ba}_2\text{PdH}_4$  crystals, and between 750 and 770 °C red-violet single crystals of  $\text{Sr}_2\text{PdH}_4$ , were obtained. Phase analyses were performed with a Guinier–Hägg focusing camera, using Si as an internal standard. The reflections were indexed with the program TREOR90,<sup>12</sup> and the least-squares refinements of the unit cell were performed with the program PIRUM.<sup>13</sup> The new hydrides,  $\text{Ba}_2\text{PdH}_4$  and  $\text{Sr}_2\text{PdH}_4$ , were found to crystallize in an orthorhombic space group, with the unit cell dimensions  $a = 8.0081(9)$  Å,  $b = 5.7688(4)$  Å, and  $c = 10.171(1)$  Å (Ba) and  $a = 7.5896(7)$  Å,  $b = 5.5084(4)$  Å, and  $c = 9.709(1)$  Å (Sr) at 293 K. Deuterated powder samples were also synthesized as described above, with unit cell dimensions  $a = 7.999(1)$  Å,  $b = 5.7620(9)$  Å, and  $c = 10.157(2)$  Å (Ba) and  $a = 7.5841(3)$  Å,  $b = 5.4975(3)$  Å, and  $c = 9.6933(5)$  Å (Sr) at 293 K.

**Single-Crystal X-ray Diffraction Data Collection, Structure Solution, and Refinement.** (a)  $\text{Ba}_2\text{PdH}_4$ . A single crystal with dimensions  $0.1 \times 0.1 \times 0.09$  mm<sup>3</sup> was mounted and sealed in a glass capillary. Single-crystal X-ray diffraction data were recorded at 150 K on a four-circle Stoe diffractometer, using Mo  $K\alpha$  radiation ( $\lambda = 0.71073$  Å). The unit cell parameters were refined from 38 well-centered reflections in the region  $27.0^\circ < 2\theta < 43.4^\circ$ . The unit cell dimensions were  $a = 7.986(2)$  Å,  $b = 5.758(2)$  Å,  $c = 10.153(4)$  Å, and  $V = 466.9(3)$  Å<sup>3</sup>. Systematic absences were consistent with space group *Pnma* (No. 62). 1336 reflections were measured, using the  $\omega$ – $2\theta$  scan technique, of which 507 were found to be unique and 400 observed. The data were corrected for Lorentz, polarization, and background effects, using the X-shape package.<sup>14</sup> A numerical absorption correction was applied, with a linear absorption coefficient of  $20.271$  mm<sup>–1</sup>. The internal *R* value after absorption correction was 0.0494.

The positions of the heavy atoms were found by direct methods (program SHELXS<sup>15</sup>). In the subsequent refinement, using the program SHELXL,<sup>16</sup> the  $\sum w(\Delta F^2)$  function was minimized with the full-matrix least-squares method. In the final refinement 20 parameters were refined, and the *R* values obtained were  $R = 0.0317$  and  $wR = 0.0650$  for all reflections. The positions of the hydrogen atoms could not be extracted from a Fourier difference map. The fractional metal-atom coordinates and anisotropic thermal parameters are listed in Table 1.

(b)  $\text{Sr}_2\text{PdH}_4$ . A crystal with dimensions  $0.32 \times 0.15 \times 0.10$  mm<sup>3</sup> was mounted and sealed in a glass capillary. Diffraction data were collected at room temperature on a Stoe image-plate diffractometer. From an examination of the reciprocal space it was concluded that the crystal was a twin with two components. X-ray intensities for the two crystallites were extracted by means of the program TWIN (Stoe IPDS). The same programs and methods as for  $\text{Ba}_2\text{PdH}_4$  were used for structure solution and model refinement. However, in the subsequent final refinement, convergence could not be attained for the anisotropic displacement parameter  $U_{22}$ . This problem may be connected with deficiencies in the obtained intensities due to difficulties in estimating correct crystal shapes. The fractional metal-atom coordinates and anisotropic thermal parameters are listed in Table 1.

## Neutron Powder Diffraction Data Collection and Hydrogen Atom Location.

(a)  $\text{Ba}_2\text{PdH}_4$ . A finely ground powder of  $\text{Ba}_2\text{PdH}_4$  was placed in an airtight vanadium container. From this sample, neutron powder diffraction data were collected at NFL, Studsvik, at 295 K using the NPD instrument, equipped with 35 He<sup>3</sup> counters. The wavelength was 1.600 Å, and data were collected between  $4.00^\circ$  to  $139.92^\circ$  in  $2\theta$ , with a step size of  $0.08^\circ$ . The Rietveld program FULLPROF<sup>17</sup> was used for profile refinement, using data in the range  $4.00^\circ < 2\theta < 94.00^\circ$ . A

(12) Werner, P.-E.; Eriksson, L.; Westdahl, M. *J. Appl. Crystallogr.* **1985**, *18*, 367.

(13) Werner, P.-E.; Eriksson, L. *World Directory of Powder Diffraction Programs*, Release 2.12, 1993.

(14) STOE, X-SHAPE revision 1.01. Crystal Optimisation For Numerical Absorption Correction; Darmstadt, Germany, 1996.

(15) Sheldrick, G. M.; SHELXL93. Program for the Refinement of Crystal Structures; University of Göttingen, Germany, 1993.

(16) Sheldrick, G. M.; SHELXS86. Program for the Solution of Crystal Structures; University of Göttingen, Germany, 1985.

(17) Rodriguez-Carvajal, J.; FULLPROF Version 3.1 Jul95-LLB-JRC, Laboratoire Leon Brillouin (CEA-CNRS), France, 1995.

**Table 1.** Fractional Atomic Coordinates and Anisotropic Thermal Parameters for Ba<sub>2</sub>PdH<sub>4</sub> and Sr<sub>2</sub>PdD<sub>4</sub> Obtained from Single-Crystal X-ray Data (Space Group *Pnma* (No. 62) with *Z* = 4; Esd's in Parentheses)

atom	position	<i>x</i>	<i>y</i>	<i>z</i>	<i>U</i> <sub>11</sub>	<i>U</i> <sub>22</sub>	<i>U</i> <sub>33</sub>	<i>U</i> <sub>13</sub>
Ba <sub>2</sub> PdH <sub>4</sub>								
Ba1	4 <i>c</i>	0.8531(1)	1/4	0.59726(9)	0.0070(5)	0.0074(5)	0.0091(5)	0.0004(4)
Ba2	4 <i>c</i>	0.0128(1)	1/4	0.16776(9)	0.0056(4)	0.0076(5)	0.0069(4)	-0.0001(3)
Pd	4 <i>c</i>	0.2598(2)	1/4	0.5808(1)	0.0088(3)	0.0082(6)	0.0089(7)	-0.0001(5)
Sr <sub>2</sub> PdD <sub>4</sub>								
Sr1	4 <i>c</i>	0.8496(3)	1/4	0.5923(2)	0.006(1)	0.000(1)	0.007(1)	-0.0002(7)
Sr2	4 <i>c</i>	0.0089(3)	1/4	0.1705(2)	0.003(2)	0.000(1)	0.006(1)	-0.0008(7)
Pd	4 <i>c</i>	0.2603(2)	1/4	0.5837(2)	0.004(1)	0.000(1)	0.005(1)	0.0015(5)

<sup>a</sup> The anisotropic thermal parameters *U*<sub>*ij*</sub> are given in Å<sup>2</sup>. *U*<sub>12</sub> and *U*<sub>23</sub> are equal to zero according to the symmetry. The data on Ba<sub>2</sub>PdH<sub>4</sub> were recorded at 150 K, and the data on Sr<sub>2</sub>PdD<sub>4</sub> at 295 K.

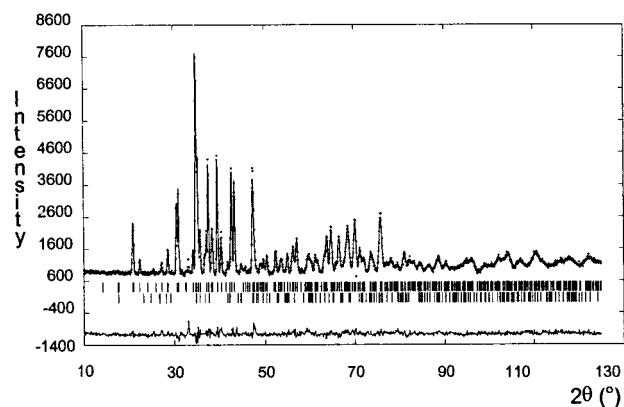
**Table 2.** Fractional Atomic Coordinates and Isotropic Thermal Parameters for Ba<sub>2</sub>PdD<sub>4</sub> and Sr<sub>2</sub>PdD<sub>4</sub> Obtained from Rietveld-Fitted Powder Neutron Diffraction Data Recorded at 295 K (Positions Are Fully Occupied; Esd's in Parentheses)

atom	position	<i>x</i>	<i>y</i>	<i>z</i>	<i>U</i> <sub>iso</sub> (Å <sup>2</sup> ) <sup>a</sup>
Ba <sub>2</sub> PdD <sub>4</sub>					
Ba1	4 <i>c</i>	0.849(2)	1/4	0.594(1)	0.010(3)
Ba2	4 <i>c</i>	0.013(2)	1/4	0.167(1)	0.003(3)
Pd	4 <i>c</i>	0.260(1)	1/4	0.581(1)	0.004(2)
D1	4 <i>c</i>	0.174(2)	1/4	0.420(1)	0.031(4)
D2	4 <i>c</i>	0.484(1)	1/4	0.608(1)	0.034(2)
D3	8 <i>d</i>	0.1779(9)	-0.007(2)	0.6599(7)	0.038(4)
Sr <sub>2</sub> PdD <sub>4</sub>					
Sr1	4 <i>c</i>	0.8505(6)	1/4	0.5924(5)	0.0068(8) <sup>a</sup>
Sr2	4 <i>c</i>	0.0060(7)	1/4	0.1703(5)	0.0068(8) <sup>a</sup>
Pd	8 <i>d</i>	0.2613(7)	1/4	0.5840(7)	0.0066(11)
D1	4 <i>c</i>	0.175(1)	1/4	0.4101(6)	0.0300(8) <sup>a</sup>
D2	4 <i>c</i>	0.4930(7)	1/4	0.6011(5)	0.0300(8) <sup>a</sup>
D3	8 <i>d</i>	0.1753(6)	-0.015(1)	0.6614(4)	0.0300(8) <sup>a</sup>

<sup>a</sup> To reduce the number of parameters when the impurity phase SrD<sub>2</sub> was included in the refinement, the isotropic thermal parameters of the two Sr positions were refined as one parameter and the same procedure was also applied to the three D positions.

Gaussian function was chosen to describe the shape of the reflections, and the background was interpolated between 16 given points. The refined positions of the heavy atoms obtained in the single-crystal refinement were included with fixed positions in the profile refinement, and thereafter the positions of the deuterium atoms were located from a three-dimensional difference Fourier map. 27 parameters (20 structural and 7 profile parameters) were refined until convergence in the final refinement. The final *R* values were *R*<sub>p</sub> = 0.0419, *R*<sub>wp</sub> = 0.0577, *R*<sub>F</sub> = 0.0696, and *R*<sub>Bragg</sub> = 0.0875. The relatively large *R*<sub>Bragg</sub> is due to accidental peculiarities of this structure refinement, as it involved a relatively large fraction of very weak reflections, which are more sensitive to errors introduced in the background correction. The polynomial background fitting included as an option in FULLPROF could not improve the refinement. The fractional atomic coordinates and isotropic thermal parameters are listed in Table 2.

(b) **Sr<sub>2</sub>PdD<sub>4</sub>**. The sample preparation and data collection were performed as described above. The program used in the profile refinement was FULLPROF98,<sup>18</sup> and neutron powder diffraction data in the region 10.00° < 2θ < 125.00° were used. A pseudo-Voigt function was used to describe the shape of the reflections, and the background was fitted by a polynomial function. The positions of the heavy atoms obtained from the single-crystal refinement of Sr<sub>2</sub>PdD<sub>4</sub> were included, and the deuterium positions were taken from the Rietveld analysis of Ba<sub>2</sub>PdD<sub>4</sub>. A small amount of unreacted SrD<sub>2</sub> was found and was refined as a second phase. To reduce the number of parameters when the SrD<sub>2</sub> was included in the refinement, the isotropic thermal parameters of strontium were refined as one parameter, and likewise the isotropic thermal parameters of deuterium. 35 parameters (24 structural and 11 profile) were refined to convergence in the final refinement. The result from the profile refinement is shown in Figure

**Figure 1.** The difference plot obtained from the Rietveld-fitted neutron diffraction data from Sr<sub>2</sub>PdD<sub>4</sub>. The observed intensities (*I*<sub>obs</sub>) are shown as circles and the calculated (*I*<sub>calc</sub>) as a line. The positions, in 2θ, of the calculated reflections of Sr<sub>2</sub>PdD<sub>4</sub> (upper) and SrD<sub>2</sub> (lower), are shown as ticks and the differences between the observed and calculated intensities are shown at the bottom.

1, and the final *R* values were *R*<sub>p</sub> = 0.034, *R*<sub>wp</sub> = 0.045, *R*<sub>Bragg</sub>(Sr<sub>2</sub>PdD<sub>4</sub>) = 0.057, and *R*<sub>F</sub>(Sr<sub>2</sub>PdD<sub>4</sub>) = 0.037. The fractional atomic coordinates and isotropic thermal parameters are listed in Table 2.

**Resistivity and AC Magnetic Susceptibility Measurements.** The electric conductivity was checked at room temperature by a four-point resistivity measurement on the powered hydride, using a specially designed tablet press with insulating ceramic walls. The static pressures applied ranged up to 2 kbar, and the input voltage ranged from 0 to 70 V. Under these conditions both Sr<sub>2</sub>PdH<sub>4</sub> and Ba<sub>2</sub>PdH<sub>4</sub> were found to be nonconducting.

AC magnetic susceptibility data were collected on both polycrystalline Sr<sub>2</sub>PdH<sub>4</sub> and Ba<sub>2</sub>PdH<sub>4</sub>, in the temperature range 12–322 K at 1000 Hz and 500 A·m<sup>-1</sup> and 500 Hz and 500 A·m<sup>-1</sup>, respectively, using a Lake Shore Inc. AC Susceptometer, model 7130, equipped with a helium cryostat. The samples were contained in a sealed glass capillary, and the experimental susceptibilities were corrected for sample-holder diamagnetism. The diamagnetic contributions from atomic core electrons were taken into account by using Pascal's constants.<sup>11</sup> From these observations we suggest that both Sr<sub>2</sub>PdH<sub>4</sub> and Ba<sub>2</sub>PdH<sub>4</sub> are diamagnetic.

## Discussion

The position of the metal atoms of the novel ternary hydrides Sr<sub>2</sub>PdH<sub>4</sub> and Ba<sub>2</sub>PdH<sub>4</sub> was found by single-crystal X-ray diffraction to correspond to the orthorhombic β-K<sub>2</sub>SO<sub>4</sub>-type structure,<sup>19</sup> with strontium(barium) and palladium in the potassium and sulfur positions, respectively. The space group is *Pnma* (No. 62), and *Z* = 4. They are also isotypic with the recently found K<sub>2</sub>ZnH<sub>4</sub>;<sup>20</sup> thus there was a strong indication that the

(19) McGinney, J. A. *Acta Crystallogr.* **1972**, B28, 2845–2851.

(18) Rodríguez-Carvajal, J. FULLPROF Version 3.5d Oct98-LLB-JRC, Laboratoire Leon Brillouin (CEA-CNRS), France, 1998.

(20) Bortz, M.; Yvon, K.; Fischer, P. *J. Alloys Compd.* **1994**, 216, 39–42.

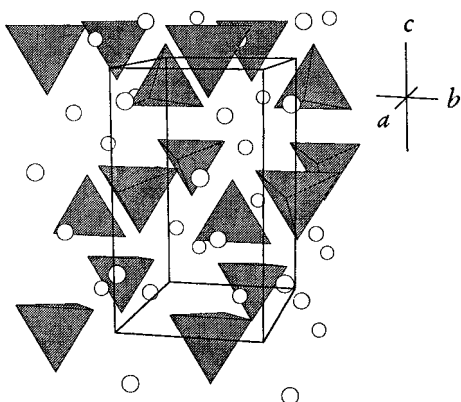


**Figure 2.** The orthorhombic structure of  $(\text{Sr,Ba})_2\text{PdD}_4$ . The  $(\text{Sr,Ba})$  atoms are shown as white spheres and the  $\text{PdH}_4$  complexes are shown as gray tetrahedra. The lattice directions and one unit cell are indicated.

**Table 3.** Shortest Interatomic Distances for the Coordination Sphere around Pd (See Figure 3) in  $\text{Ba}_2\text{PdD}_4$  and  $\text{Sr}_2\text{PdD}_4$  Obtained from Neutron Powder Diffraction Data at Room Temperature (Esd's in Parentheses)

atoms <sup>a</sup>	$\text{Ba}_2\text{PdD}_4$	$\text{Sr}_2\text{PdD}_4$	
	distances (Å)		
Pd–D1	1.78(1)	1.809(9)	intra
D2	1.81(1)	1.764(8)	intra
D3, D3b	1.809(9)	1.766(6)	intra
A''2	3.23(1)	3.086(8)	
A''1	3.29(1)	3.117(7)	
D3–A''2	2.72(1)	2.493(6)	
D2–A''2	2.80(1)	2.633(7)	
D1–A''2	2.86(2)	2.653(8)	
D1–D3, D3b	2.85(1)	2.839(7)	intra
D1–D2	3.13(1)	3.042(9)	intra
D3–D3b	2.96(1)	2.918(8)	intra
D2–D3, D3b	2.91(1)	2.876(7)	intra
A''1–A''2	3.93(1)	3.648(7)	
	intramolecular angles (deg)		
D1–Pd–D3, D3b	105.6(4)	105.2(3)	
D1–Pd–D2	121.7(7)	116.7(5)	
D3–Pd–D3b	110.1(6)	111.5(4)	
D2–Pd–D3, D3b	106.8(4)	109.1(3)	

<sup>a</sup> "A" indicates the alkaline-earth metal atom.

hydride contains novel tetrahedral anionic  $\text{Pd}(0)\text{H}_4$  complexes. The existence of tetrahedral  $\text{PdD}_4$  complexes was confirmed by neutron powder diffraction experiments on deuterated samples (Figure 2). Hydrogen occupies three crystallographically different positions in the structure, involving three different Pd–D distances (Tables 2 and 3), with an average value of 1.80 (Ba) and 1.78 Å (Sr). The palladium–deuterium complexes are counterbalanced by Sr or Ba atoms surrounding each complex in a disordered tricapped cubic configuration (Figure 3). The closest Ba–D and Sr–D distances are 2.71 and 2.49 Å, respectively, which is slightly longer than the shortest distances found in  $\text{BaD}_2$ <sup>21</sup> and  $\text{SrD}_2$ ,<sup>22</sup> and the shortest Ba–Ba and Sr–Sr are 3.93 and 3.65 Å, respectively, which is slightly shorter than the distances in the corresponding binary deuterides. The  $\text{PdD}_4$  tetrahedra are distorted, with D–Pd–D bond angles ranging from 105.6° to 121.7° (Ba) and 105.2° to 116.7° (Sr). The closest D–D distance (intermolecular) is 2.80 Å in  $\text{Ba}_2\text{PdD}_4$  and 2.58 Å in  $\text{Sr}_2\text{PdD}_4$ , and the closest intramolecular D–D distance is 2.85 Å ranging up to 3.13 Å in  $\text{Ba}_2\text{PdD}_4$  and 2.84 Å ranging up to 3.05 Å in the strontium analogue.

(21) Bronger, W.; Chi Chien, S.; Müller, P. *Z. Anorg. Allg. Chem.* **1987**, *545*, 69–74.

(22) Brese, N. E.; O'Keeffe, M.; von Dreele, R. B. *J. Solid State Chem.* **1990**, *88*, 571–576.

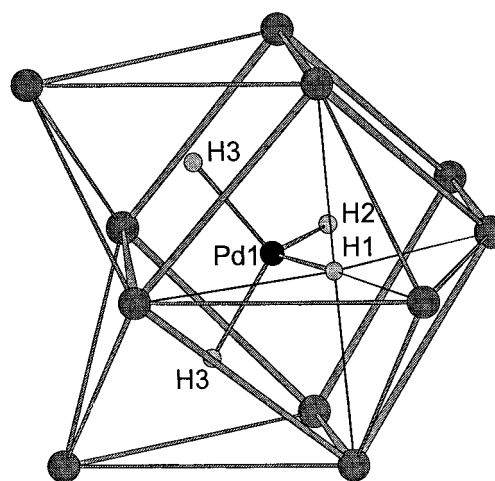


**Figure 3.** The coordination sphere around one Pd atom, with the four hydrogen atoms connected, forming a distorted tetrahedron. Alternatively, the structures may be regarded as interstitial hydrides with hydrogen located in octahedral holes, each formed by 5  $(\text{Sr,Ba})$  atoms and one Pd atom.

The diamagnetism and nonconducting properties favor a molecular description of the bonding in the  $\text{Pd}(0)\text{H}_4$  complex, with an 18-electron counting rule making it isoelectronic with the tetrahedral, anionic  $\text{Ni}(0)\text{H}_4$  complexes found in  $\text{Mg}_2\text{NiH}_4$ ,  $\text{Cu}(I)\text{H}_4$  found in  $\text{Ba}_7\text{Cu}_3\text{H}_{17}$ ,<sup>23</sup> and  $\text{Zn}(II)\text{H}_4$  found in  $\text{K}_2\text{ZnH}_4$ . But on the other hand, as shown in Figure 3, the structure of  $\text{A}_2\text{PdH}_4$  ( $\text{A} = \text{Sr, Ba}$ ) certainly has some similarities to interstitial hydrides with hydrogen in octahedral sites coordinated by one palladium atom and five barium atoms.

In  $\text{Ba}_2\text{PdH}_4$  and  $\text{Sr}_2\text{PdH}_4$  the Pd–H bond is long, with an average of 1.80 Å (Ba) and 1.78 Å (Sr), as compared to 1.61 Å in  $\text{Na}_2\text{PdH}_4$ , 1.63 Å in  $\text{K}_2\text{PdH}_4$ ,<sup>24</sup> 1.68 Å in  $\text{A}_2\text{PdH}_4$  ( $\text{A} = \text{Li, Na}$ ) and 1.72 Å in  $\text{NaBaPdH}_3$ . This indicates a weak bond to palladium, more in agreement with the 1.83 Å Pd–H distance in  $\text{NaPd}_3\text{H}_2$ .<sup>25</sup>  $\text{NaPd}_3\text{H}_2$  has a metal-atom structure almost identical with that of the interstitial palladium hydride, but with sodium substituting for one-fourth of the palladium atoms, thus creating a superstructure based on the FCC palladium lattice. Hydrogen fully occupies the octahedral site coordinated by one sodium and five palladium atoms, leaving the other octahedral site empty. Here, hydrogen again forms a  $\text{PdH}_2$  dumbbell similar to that in  $\text{Na}_2\text{PdH}_2$ , but with a prolonged Pd–H bond.  $\text{NaPd}_3\text{H}_2$  has electrical properties similar to palladium hydride, and it is also a low-temperature superconductor.<sup>26</sup>

The insulating properties of  $\text{A}_2\text{PdH}_4$  ( $\text{A} = \text{Sr, Ba}$ ) systems support a molecular description, however. With reference to the classification by Firman and Landis of hydrogen as bonded in TM–hydrogen complexes or in interstitial sites outside the TM coordination sphere, the  $\text{A}_2\text{PdH}_4$  ( $\text{A} = \text{Sr, Ba}$ ) hydrides clearly are interesting intermediate cases. On one hand, there is a  $\text{PdH}_4$  complex, albeit with a long and weakened Pd–H bond; on the other hand, they are close to being interstitial hydrides, but with the interstitial site coordinating one palladium atom.

The discovery of yet another palladium–hydrogen complex with formally zerovalent palladium again emphasizes the ability of hydrogen to stabilize electron-rich complexes, despite a

(23) Huang, B.; Fauth, F.; Yvon, K. *J. Alloys Compd.* **1996**, *244*, L1–L4.

(24) Kadir, K.; Kritikos, M.; Noréus, D.; Andresen, A. F. *J. Less Common Met.* **1991**, *36*, 172–174.

(25) Kadir, K.; Noréus, D. *Z. Phys. Chem.* **1993**, *179*, 249–253.

(26) Kadir, K.; Lundquist, P.; Noréus, D.; Rapp, Ö. *Solid-state Commun.* **1993**, *88*, 891–893.

mechanism lacking for conventional back-donation. We attribute this to the large polarizability of the TM–hydrogen bond, which permits hydrogen to distribute electron density away from the proximity of the central atoms by means of its potential to adopt a larger radius. It should be remembered that the real electron population in the valence shell of a transition metal, irrespective of the formal oxidation state, is very like that of its atomic state and it is thus likely that this small electron-accepting capacity (in absolute terms) is enough to stabilize the central atom in what conventionally would correspond to a low formal oxidation state. A flexibility in the bond mechanism is also reflected in the ease with which different coordinations are formed in response to the number of electrons supplied by the surrounding electropositive metal atoms in the series  $A_2PdH_2$  ( $A = Li, Na$ ),  $NaBaPdH_3$ , and  $A_2PdH_4$  ( $A = Sr, Ba$ ).

Hydrogen can adopt any coordination geometry, since the s-orbital is spherical and totally symmetric. With reference to Pearson's unique softness of  $H^-$ , the low resistance to deformation of the electron density combined with the support from the local cation framework will allow for a number of energetically similar structures to be possible in these systems. This flexibility and adaptability of hydrogen makes it important to consider the total electronic structure of the metal atom lattice for understanding the stability of the different hydrides.

The influence from the cations upon the formation of different TM coordinations is thus strong, and this is probably the reason the structures deviate from the general framework developed by Firman and Landis for this type of hydride. For a more complete description of this electron-rich complex the counterions have to be included in the quantum-chemical calculation in a more detailed manner.

There are, however, further differences in the role of the counterions in the palladium series. With only two hydrogens attached to palladium to help distributing the electron density, and with small cations, the lithium and sodium counterions are forced to retain some valence electron density, giving metallic properties to the hydrides. The metallic properties and stabilization of the similar system  $Mg_3RuH_3$  have recently been discussed by Hoffman et al.<sup>27</sup>

This dependence of the formation and stability of the complex on the surrounding lattice could have technological implications, similar to the alloying of interstitial hydrides for battery applications to modify the hydrogen storage characteristics.

(27) Miller, G. J.; Deng, H.; Hoffmann, R. *Inorg. Chem.* **1994**, *33*, 1330–1339.

(28) Noréus, D.; Kihlberg, L. *J. Less Common Met.* **1986**, *123*, 233–239.

(29) Guthrie, S. E.; Thomas, G. J.; Noréus, D.; Rönnebro, E. *Materials Research Society Symposium Proceedings Series*, Vol. 513.

(30) Orimo, S.; Ikeda, K.; Fujii, H.; Fujikawa, Y.; Kitano, Y.; Yamamoto, K. *Acta Mater.* **1997**, *45*, 2271–2278.

(31) Kohno, T.; Tsuruta, S.; Kanda, M. *J. Electrochem. Soc.* **1996**, *143*, L198–L199.

(32) Orimo, S.; Ikeda, K.; Fujii, H.; Saruki, S.; Fukunaga, T.; Züttel, A.; Schlapbach, L. *Acta Mater.* **1998**, *46*, 4519–4525.

In  $Mg_2NiH_4$ , which contains a nickel analogue of the complex presented here, this has already been observed.  $Mg_2NiH_4$  exhibit a twinning phenomenon on the unit cell level that stabilizes the hydride. If the twinning is suppressed the stability of the hydride is decreased, making it more suitable for hydrogen storage.<sup>28,29</sup>

Related to this is probably also the recently reported  $MgNiH_{1.9}$  system,<sup>30</sup> which is presently the target of intense investigations by battery researchers as it is claimed to have almost twice the storage capacity of the conventional battery alloys.<sup>31</sup> The new compound is made by mechanical alloying of  $Mg_2Ni$  with more nickel until a homogeneous, but amorphous 1:1 mixture of  $MgNi$  composition is obtained. As both alloy and hydride are amorphous, no conventional structure determination has been made. Orimo et al. have, however, reported the radial distribution function of the interatomic distances obtained from a neutron diffraction experiment on the deuteride. Without referring to a molecular description of the bonding, a Ni–D distance of  $1.64 \pm 0.03$  Å and a coordination number of  $1.7 \pm 0.3$  for the D atoms around Ni are given.<sup>32</sup> With reference to the  $A_2PdH_2$  ( $A = Li, Na$ ) systems, this bond distance could indicate the existence of a  $NiH_2$  complex counterbalanced by a disordered Mg–cation arrangement.

Anyway, we hope that our work in synthesizing and characterizing the palladium systems may open up possibilities of obtaining also the nickel-based analogues, which might, apart from a better fundamental understanding of the metal–hydrogen bond, also lead to better and more practical storage systems.

## Conclusions

The addition of a third zerovalent-palladium hydrido complex in the series  $A_2PdH_2$  ( $A = Li, Na$ ),  $NaBaPdH_3$ , and  $A_2PdH_4$  ( $A = Sr, Ba$ ) shows that hydrogen as a ligand can participate in the stabilization of such a formally low oxidation state, where one would only expect good electron accepting ligands to be involved. The large variation in hydrogen coordination numbers and geometries in response to the s-metal counterion charge distribution implies that the unique chemical softness of  $H^-$  permits stabilization of a number of probably energetically similar structural configurations in these systems. It also indicates the need to consider the total metal lattice when explaining the stability of the different complexes.

**Acknowledgment.** We thank Håkan Rundlöf, NFL, Studsvik, Sweden, for collecting the powder neutron diffraction data. This work was financially supported by the Swedish Research Council for Engineering Sciences (TFR).

**Supporting Information Available:** Table of experimental  $\chi_M$  values of  $Ba_2PdH_4$  and  $Sr_2PdH_4$  (PDF). This material is available free of charge via the Internet at <http://pubs.acs.org>.

JA991047R